Electronic Supplementary Material (ESI) for Soft Matter.


# Electronic Supplementary Information

# The relation between local density and bond-orientational order during crystallization of Gaussian core model

Yan-Wei Li[ac] and Zhao-Yan Sun[ab*]

E-mail: zysun@ciac.ac.cn

*a State Key Laboratory of Polymer Physics and Chemistry, Changchun Institute of Applied Chemistry, Chinese Academy of Sciences, Changchun 130022, China.*

*b Xinjiang Laboratory of Phase Transitions and Microstructures in Condensed Matters, College of Physical Science and Technology, Yili Normal University, Yining, 835000, China.*

*c Dutch Polymer Institute (DPI), PO Box 902, Eindhoven, 5600 AX, The Netherlands.*

*To whom correspondence should be addressed

To test the generality of our results, we perform molecular dynamics simulation of Lennard-Jones (LJ) particles in the $NPT$ ensemble at $T = 0.7$. We simulate $N = 13500$ LJ particles with interaction potential between particles given by $U(r) = 4\varepsilon[(\sigma/r)^{12} - (\sigma/r)^{6}]$. The LJ interaction parameters are $\sigma = 1.0$, and $\varepsilon = 1.0$. The potential is truncated and shifted at $2.5\sigma$. All the particles have the same mass $m$. Length, energy and time are reported in units of $\sigma$, $\varepsilon$ and $\sqrt{m\sigma^2/\varepsilon}$, respectively. We compress the system from $P = 0.5$ to $P = 5.0$ at $T = 0.7$ by an interval of 0.3. In each interval, $2.0 \times 10^7$ and $1.0 \times 10^7$ time steps are used to equilibrium and sample, respectively.

We first investigate structure changes in the compressing process of LJ system. The probability distributions of $W_6$ and $W_4$ are shown in Fig. S1. When the pressure is in the range from $P = 0.5$ to $P = 4.4$, the system is in the fluid state and no crystal structure has been found. When the pressure increases to $P = 4.7$, we can obtain the fluid to solid transition, and the system shows a strong tendency to form an fcc-like structure.

The variation of the potential energy $U$ and that of the number averaged cluster size $< N_{c,dense} >$ and $< N_{c,order} >$ are shown in Fig. S2. Clearly, sharp changes of the three curves occur at $P =$ 4.7 (denoted by the cyan dashed line in Fig. S2), implying that the first-order phase transition occurs, and this result is consistent with that in Fig. S1. It also shows that the number averaged cluster size $< N_{c,dense} >$ and $< N_{c,order} >$ can characterize the liquid-crystal transition, which is consistent with our results of Gaussian core model in the main text (see Fig. 3 in the main text). Consistent with the results of Fig. 3(b) in the main text, the value of $< N_{c,dense} >$ is larger than that of $< N_{c,order} >$ for both liquid and fcc-favored solid phases. This result is different from Fig. 3(a) in the main text, where $< N_{c,order} >$ is larger than $< N_{c,dense} >$ in the bcc-favored solid phase. We infer that the values of $< N_{c,dense} >$ and $< N_{c,order} >$ are quantitatively affected by the structure of different polymorphs in the solid phase. Nevertheless, the spatial correlations of both densely packed particles and highly bond-ordered particles both become stronger when crystallization occurs, and both of them can be used as the characterization methods of the liquid-crystal transition.

To investigate the nucleation process, we track the trajectory of each particle at around the

crystallization transition point ($T = 0.7$ and $P = 4.7$) of LJ system. We show in Fig. S3 the solid bond number $\xi$ in $q_6$-$\rho$ plane and in $\overline{q}_6$-$\rho$ plane for $t = 10695$, $t = 10755$ and $t = 12020$ at the state point $T = 0.7$ and $P = 4.7$. Consistent with the results of Gaussian system shown in Fig. 6 and Fig. 7 in the main text, nucleation also starts from the region with high bond-orientational order in the LJ system (see the distribution of particles with high $\xi$ in Fig. S3(a) and in Fig. S3(d)).

Similar to Fig. 8 in the main text, we also show in Fig. S4 the time evolution of the crystal fraction $X = N_{solid}/N$ and that of the Spearman correlation coefficients $K(\rho, q_6)$ and $K(\rho, \overline{q}_6)$ for $T = 0.7$ and $P = 4.7$ of LJ system. $K(\rho, q_6)$ of LJ system shows clear crystal fraction dependence, which is also consistent with the Gaussian system. Different from Fig. 8(a) in the main text, $K(\rho, q_6)$ goes to $\sim 0.15$ rather than $\sim 0$ after the crystallization has finished. We infer that the thermal fluctuation in LJ system is not so large as Gaussian system, and this leads to weak correlation between $\rho$ and $q_6$ even in the solid phase. Similar to the result of Fig. 8(b) in the main text, the correlation between $\rho$ and $\overline{q}_6$ is weak in the fluid and solid phases (see blue triangles in Fig. S4). However, we see obvious increase in $K(\rho, \overline{q}_6)$ during the crystal growth stage. This is because both liquid and solid phases exist in this stage. Moreover, the average density of solid phase (the position of the black dashed line in Fig. S3(e)) is larger than that of liquid phase (the position of the white dashed line in Fig. S3(e)) in the LJ system, and so does $\overline{q}_6$ (see Fig. S3(e)). This leads to relatively large value of $K(\rho, \overline{q}_6)$ in the crystal growth stage of the whole system, which is probably due to the differences of $\rho$ and $\overline{q}_6$ between different phases (liquid and solid), but not the increase of the correlation between $\rho$ and $\overline{q}_6$ of the system. However, this phenomenon does not exist in Gaussian system (see Fig. 7 and Fig. 8(b) in the main text). This is because that the thermal fluctuation is large in the soft spheres system, and the differences of the average density between liquid and solid phase are very small.

From above discussions, we can see that the main conclusions obtained from Gaussian system in the main text are quite similar to the results of LJ system.

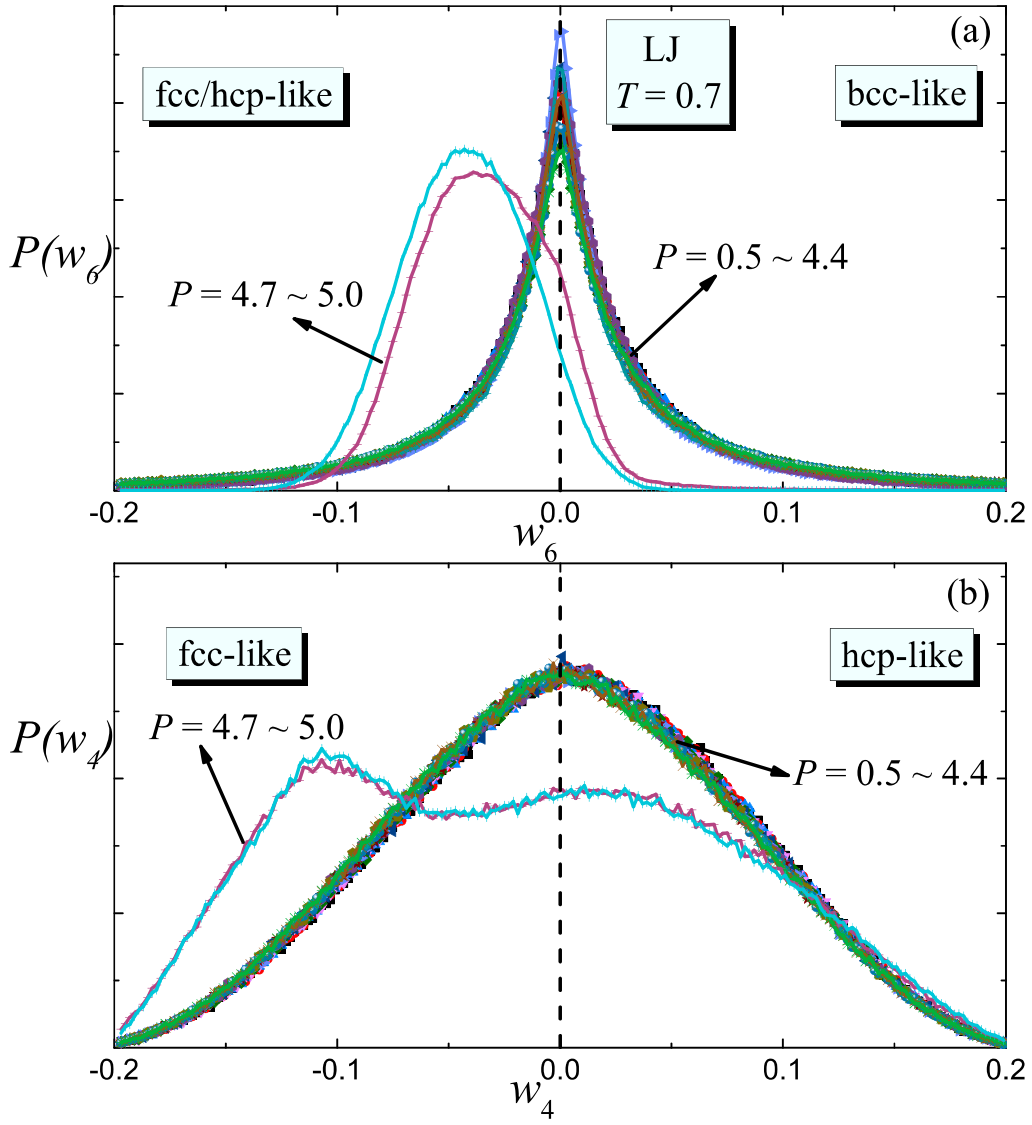


Fig. S1: (a) $W_6$ probability distribution and (b) $W_4$ probability distribution at different pressures for $T = 0.7$ of LJ system.

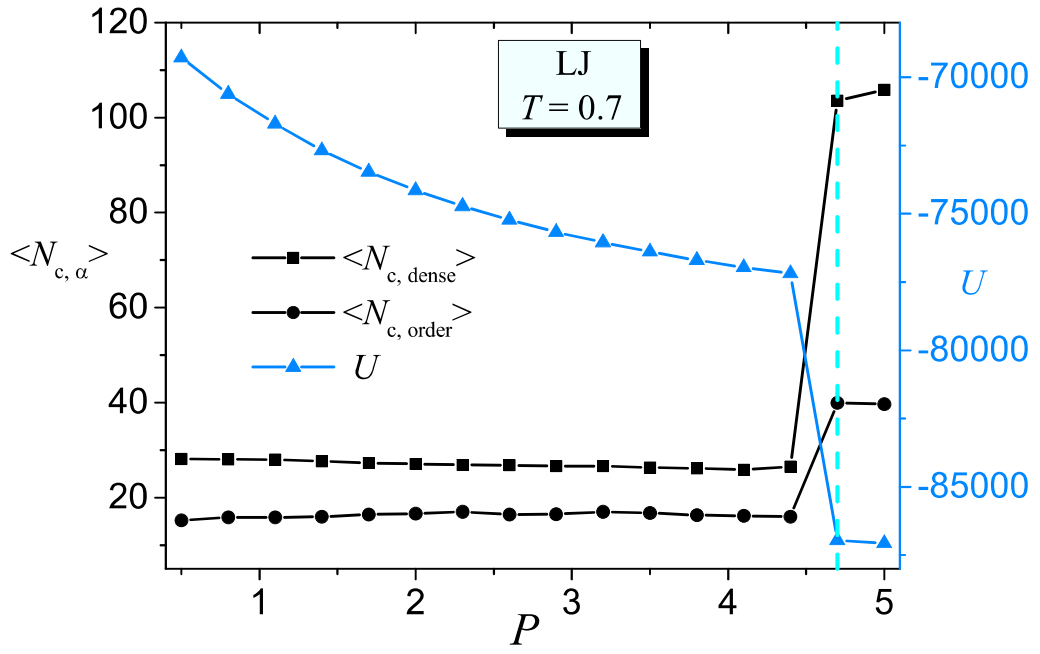


Fig. S2: Pressure dependence of number averaged cluster size $< N_{c,dense} >$ (black squares) and $< N_{c,order} >$ (black circles) and pressure dependence of the potential energy $U$ (blue triangles) at $T = 0.7$ for LJ system. Throughout pressing the system from $P = 0.5$ to $P = 5.0$, sharp variations can be seen in all the three curves, signifying a first-order phase transition (marked by the cyan dashed line).

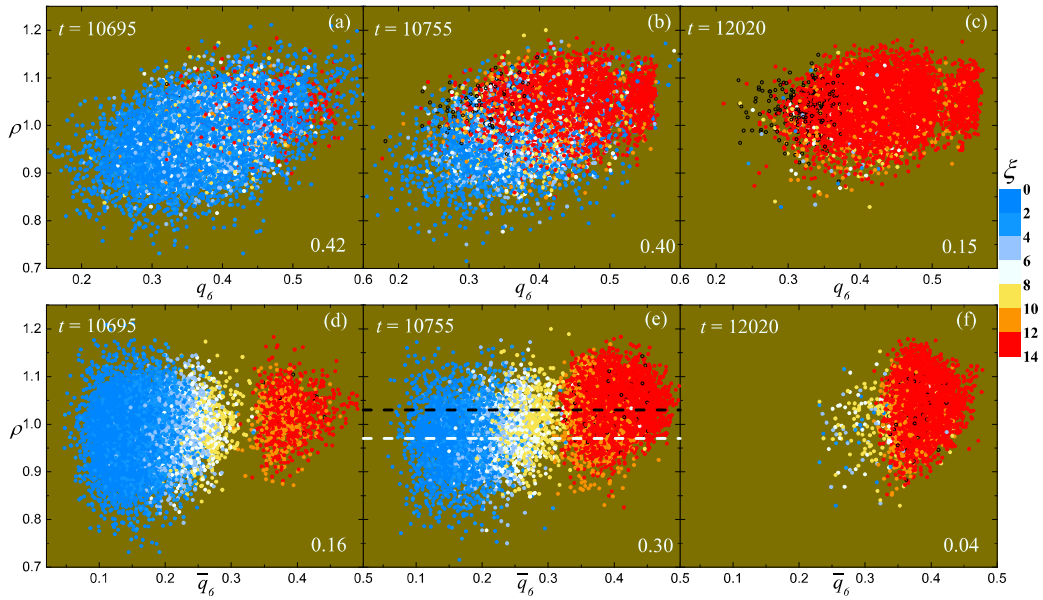


Fig. S3: The solid bond number $\xi$ for all particles of the system in the $q_6$-$\rho$ plane ((a), (b) and (c)) and in the $\overline{q}_6$-$\rho$ plane ((d), (e) and (f)) for the state point $T = 0.7$ and $P = 4.7$ of LJ system. Here, $\xi$ grows from 0 to 14 from the liquid to the crystal phase and is represented by the color of each symbol. Numbers at the lower right indicate Spearman rank correlation coefficients $K(\rho, q_6)$ (in (a), (b) and (c)) and $K(\rho, \overline{q}_6)$ (in (d), (e) and (f)). The time for each histogram is shown at the top left of each one. The black (white) dashed line in (e) marks the average density of solid (liquid) phase, which is simply used to guide the eye.

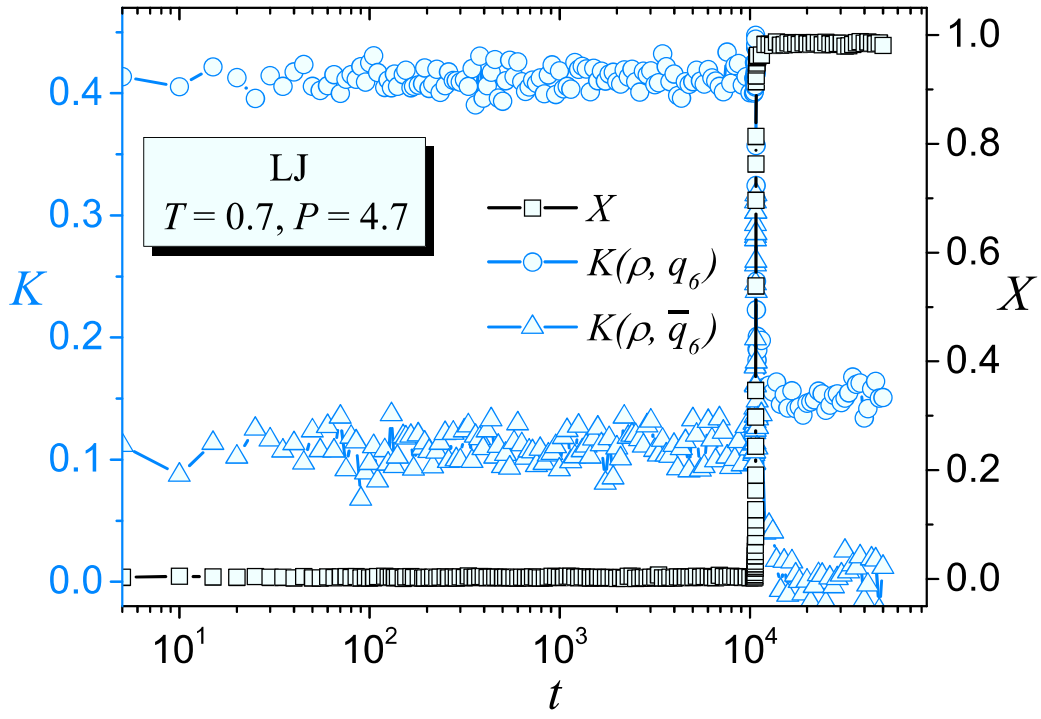


Fig. S4: Time evolution of the crystal fraction $X = N_{solid}/N$ (black squares) and that of the Spearman rank correlation coefficients $K(\rho, q_6)$ (blue circles) and $K(\rho, \overline{q}_6)$ (blue triangles) for the state point $T = 0.7$ and $P = 4.7$ of LJ system.